



Mineralogical Characteristics and Estimating the Depth of the Formation of Gabbroic Rocks in Dehsard area (Southeast of Iran)

Mehdi Ebrahimnejad^{1*}, Mohsen Arvin², Sara Dargahi³

¹ Ph.D. Student, Department of Geology, College of Sciences, Shahid Bahonar University of Kerman, Kerman, Iran.

² Professor, Department of Geology, College of Sciences, Shahid Bahonar University of Kerman, Kerman, Iran.

³ Associate professor, Department of Geology, College of Sciences, Shahid Bahonar University of Kerman, Kerman, Iran.

ABSTRACT

The upper Triassic gabbroic magmatism is located in the southernmost of the Sanandaj-Sirjan zone, in the southwest of Kerman, Iran. Based on field observations and petrographic studies, this mafic body is Hornblende-gabbro. The general texture of the samples is hypidiomorphic granular; but porphyry, intergranular and poikilitic textures also occasionally occur in mafic samples. Mineralogically the gabbroic rocks include plagioclase, clinopyroxene, amphibole, titanite, apatite, epidote, calcite, and chlorite. Mineral chemistry studies demonstrate that the composition of plagioclases is albite to oligoclase and clinopyroxenes are composed of diopsides. The composition of clinopyroxenes includes an iron-magnesium-calcium type. The amphiboles are calcic and plotted in the magnesium hornblende and actinolite field. The petrogenesis of parental magma is the arc type related to the subduction environment. Based on geothermobarometry studies on amphiboles and clinopyroxenes, the average temperatures of 1000-1200 °C with pressure ranges of 2.05 to 5.58 Kbar were estimated for gabbroic samples. The calculated pressures are equivalent to near the surface conditions to the depth of approximately 14 km.

Keywords: Geothermobarometry; Gabbro; Clinopyroxene; Amphibole; subduction

Corresponding author: Mehdi Ebrahimnejad

e-mail ✉ Mehdi.geo2015@gmail.com

Received: 14 December 2019

Accepted: 21 June 2020

1. INTRODUCTION

The Sanandaj-Sirjan Zone, 1500 km long, consists of Mesozoic sedimentary volcanic rocks and plutonic complexes with multiple metamorphic ones (Berberian and King, 1981; Mohajjel et al., 2003; Nazemei et al., 2018). The connection between the Arabian Plateau and the subcontinent of central Iran is distinguishable by the two dismembered ophiolitic complexes of Nairiz and Kermanshah (in Fars and Lorestan province, respectively) in the southern part of the Sanandaj-Sirjan zone (Stocklin et al., 1968; Arvin et al., 2007; Azizi et al., 2011). The Sanandaj-Sirjan zone and its plutonic units have been the subject of numerous petrological, structural, and geological studies (Sedighian et al., 2017; Deevsalar et al., 2018). Mesozoic gabbroic bodies are formed due to the subduction of the Neo-tethys oceanic crust beneath the Sanandaj-Sirjan zone in south-central Iran (Shahbazi et al., 2010; Mohammadi et al., 2013). The most important genesis areas of gabbros are ocean expansion centers, oceanic islands, continental rifts, and subduction areas (Gill, 2010). The gabbros are divided into different varieties based on the composition of the mineralogy, wherein 'Dehsard' region, according to the percentage of the

major minerals, plagioclase, pyroxene, and amphibole; the studied gabbroic body is hornblende gabbro. The chemical composition of rock minerals follows the host rock magmatic series (Zhu and Ogasawara, 2004; Avanzinelli et al., 2004), so studying the chemistry of minerals helps to understand the magmatic processes. The magmatic evolution of the host rock is specified by investigation of the crystallization conditions and the processes affecting mineral crystallization (Molina et al., 2009). This study attempts to discover the temperature and crystallization pressure conditions of these minerals by using the chemical data of pyroxene and plagioclase minerals of the studied gabbro and to investigate the tectonic origin of the gabbros of Dehsard region.

Geological setting

Since the Iranian plateau is considered part of the Alpine-Himalayan orogenic belt, the opening and closing of the paleo-tethys and Neo-tethys oceans play an important role in geological evolution (Berberian, 2014). Sanandaj-Sirjan zone is the most complex structural area of Iran (Falcon, 1974; Omrani et al., 2008). The major events of the metamorphism and magmatism of the Sanandaj-Sirjan zone have been attributed to the Mesozoic (Sepahi and Athari, 2006; Baharifar et al., 2004). The plutonic bodies of Dehsard region with the age of upper Triassic in 230 km southwest of Kerman and in the

southernmost part of Sanandaj-Sirjan zone, are located between latitudes 56° 25' - 56° 35' east and latitudes 28° 45' - 28° 33' north (Fig. 1) (Nazemzadeh and Rashidi, 2006). Layered condition in some rocks in the region is observed due to the sequence of felsic and mafic bodies (Fig. 2a). The mafic body in the region includes the Hornblende gabbro, and the felsic phase includes granitoid rocks. In some cases, the felsic phase of the investigated region has injected into the mafic phase in form of dike and in some cases, it has a distinct boundary with the mafic phase (Fig. 2a,b). The aplite veins, which indicate the final phase of magmatic crystallization, also expose outcrop in the region.

2. ANALYSIS METHODS

Field studies were performed by selecting the appropriate sampling. Afterward, by selecting appropriate samples and preparing microscopic sections and petrographic studies, in order to provide an accurate recognition and investigation of pyroxene and plagioclase minerals in the investigated gabbros, electron microprobe analysis was performed on the minerals by JEOL-JX8600M electron microprobe device with accelerating voltage conditions of 15 kW and 2 × 8-10 amp radiant current, in Earth Sciences Department of Yamagata University, Japan. The analysis time of each point varied from 30 seconds to 5 minutes, depending on the type of mineral and the elements required for analysis. The normalization standards for these minerals are apatite, wollastonite, albite, adularia, laboratory SiO₂, CaF₂, MgO, MnO, Fe₂O₃, Al₂O₃, TiO₂, and NaCl. The results are presented in Tables 1 to 3, respectively.

Petrography

The studied gabbroic rocks in the macroscopic samples are dark gray to black. The predominant texture of these rocks is granular and intergranular (Fig. 2c,e). The porphyry and poikilitic textures are also found in them. The composition of these rocks is Hornblende gabbro. The main mineralogical compositions of them are plagioclase, clinopyroxene, and amphibole. The other existing minerals are apatite, titanite, epidote, calcite, and chlorite (Fig. 2). Plagioclase is the most abundant major mineral in these rocks (25 to 55 wt.%). The plagioclases are euhedral to subhedral. In some of them sericitic alteration are occurred. The amphibols in these rocks are Hornblende and actinolite (10 to 35 wt. %), the cleavage of Hornblende is well visible in these minerals. Clinopyroxenes are anhedral to subhedral and include 10 to 30 wt.% of studied rocks.

Mineral chemistry

Plagioclase: This mineral is the major mineral in the studied gabbroic rocks. The structural formula of plagioclase is calculated based on 8 oxygen and the result of the analysis of these minerals is presented in Table 1. According to the results of the analysis, the composition of the plagioclase in the investigated gabbro is albite to oligoclase (Fig. 3a). The anorthite contents of plagioclase vary from An_{1.35} to An_{10.65}. There is no zoning in plagioclases, which indicates a balanced growth during crystallization of the studied plagioclase minerals (Shelley, 1993).

Pyroxene: The composition of the pyroxenes is En_{1.90}Fs_{6.97}Wo_{28.95} to En_{53.59}Fs_{25.21}Wo_{72.88}. The structural formula of pyroxenes is based on six oxygen atoms and four cations, as shown in Table 2. According to the classification of Murimoto et al. (1988), the investigated pyroxenes are rich in calcium (average 0.82 wt.%) and poor in sodium (less than 0.43 wt.%). The studied pyroxenes plot in the diopside area in the Wollastonite-enstatite-ferrosilite diagram (Fig. 3b). In the Ti-Na-Al^{IV} diagram, most of the studied clinopyroxenes have a mole percentage CATS (Ca-Tschermak's molecule) of more than 50% and are enriched with calcium (CATS) (Fig. 3c) (Papke et al., 1974). According to the diagram J-Q (Morimoto, 1988), the studied pyroxenes are the clinopyroxenes Ca-Mg-Fe (Quad) type (Fig. 3d). According to the values of Ti, Cr, and Na (0.00 to 0.35, 0, and 0.01 to 0.43, respectively) and the Al^{tot} vs Ti+Cr+Na diagram, the studied pyroxenes are magmatic pyroxenes (Fig. 3e) (Berger et al., 2005). Clinopyroxenes with magnesium number of less than 86% indicate the separation of crystals from magma (Le Bas et al., 1962; Deer et al., 1992), the magnesium number of the studied samples (average of 81%) confirms that these samples are magmatic.

Amphibole: Amphibole is another major mineral in the studied rocks. The results of their structural formula according to the standard formula of amphibole AB₂C₅^{IV}T₈O₂₂(OH)₂ (Leake et al., 1997) based on 23 oxygen and 13 cations in tetrahedron and octahedron position are presented in Table 3. According to B_{Ca} (1.86 to 1.91) and B_{Na} (0.8 to 0.13), amphiboles are calcic (Fig. 4a) and in the (Le Bas et al., 1962) diagram, the studied amphiboles are plotted in the actinolite to magnesium hornblende (Fig. 4b). (Sial et al., 1998) presented a diagram that distinguishes magmatic amphiboles from metamorphic. According to this diagram, the primary amphiboles in the studied gabbro are magmatic type (Fig. 4c) (Leake et al., 1997) believe that the Si values of magmatic amphiboles were less than 7.3, while amphiboles with silica above 7.3 were formed from processes below the freezing line (Agemar et al., 1999; Chivas et al., 1982).

Oxygen fugacity and estimate of magmatic water

Oxygen fugacity has a significant effect on magmatic processes, crystallization sequence, and the type of crystallized minerals, and the amount of oxygen fugacity depends on the Magma's tectonic environment. In the Al^{VI}+2Ti+Cr diagram vs. Al^{IV}+Na (Schweitzer et al., 1979), the studied samples are plotted below the Fe⁺³=0 line that indicates the crystallization of the studied pyroxenes in the low oxygen fugacity. In this diagram, if the samples locate above that line, it indicates the oxygen fugacity is high. In fact, the greater or lesser the distance of the samples from the Fe⁺³=0 equilibrium line shows the greater or lesser the oxygen fugacity in the clinopyroxene crystallization environment (Fig. 5a).

The Al^{IV} distribution is used in the octahedron and tetrahedron position for estimating the magmatic water and the pressure. An increase in the amount of Al^{IV} indicates a decrease in the amount of water in the crystallization environment of pyroxene (Helz, 1973). According to the Al^{VI} vs Al^{IV} diagram, the pressure of studied pyroxenes is 5Kbar and the water content of 10% (Fig. 5b).

Determining the magma series and the tectonic environment

The chemical composition and origin of the constituent magma affect the chemical composition of clinopyroxenes (Kamenetsky et al., 2001). As a result, the chemical composition of pyroxene can be used to understand the magmatic series and the tectonic environment of the host magma (Letierrier et al., 1982; Beccaluva et al., 1989). Using diagrams of Al_2O_3 vs. SiO_2 , it is distinguished that the magma constituent of the investigated minerals is sub-alkaline (Fig. 6a). In the TiO_2 diagram against Al_2O_3 , the studied clinopyroxenes are located within the calc-alkaline range (Fig. 6b). In the TiO_2 diagram vs. Al_2O_3 and MgO , the studied amphiboles are also located in the sub-alkaline range (Fig. 6c,d).

Numerous diagrams have been designed to investigate the tectonic environment of gabbroic masses based on the clinopyroxene minerals. (Letierrier et al., 1982) presented a diagram based on the $Ti + Cr$ vs. Ca , which distinguishes the clinopyroxenes of the Mid-ocean ridge and tholeiitic environment from the clinopyroxenes of the volcanic arc environment. According to this diagram, the investigated clinopyroxenes are formed in a volcanic arc environment (Fig. 7a). Also in diagram F_1 - F_2 (Nisbet and Pearce, 1977), which is designed based on a combination of the oxides of all the major and minor elements of clinopyroxenes to differentiate the tectonic environment of basalts, the clinopyroxenes of the Dehsard gabbroic body are located in the volcanic arc basalts (Fig. 7b). (Beccaluva et al., 1989) believes that pyroxenes crystallized from volcanic-related magma have high SiO_2 and low Ti , so the studied clinopyroxenes are formed in the volcanic arc environment (Table 2). In the TiO_2 diagram vs. $Al^{IV} \cdot 100/2$ (Al_2) (Loucks, 1990), the studied pyroxenes are plotted in the subduction zone. In this diagram, the subduction environment is distinguished from the environment associated with ophiolite and rift (Fig. 7c). In the diagram (Coltorti et al., 2007), which was provided for the tectonic environment of amphiboles, the studied amphiboles are plotted in the subduction environment (Fig. 7d).

Thermometry – Barometry

Given that the combination of clinopyroxenes is associated with changes in temperature and pressure, the mineral can be used to estimate temperature and crystallization pressure (Sadeghian and Minggu, 2019; Bindi et al., 1999; Aydin et al., 2009). For thermometry of mono mineral clinopyroxene by drawing method (Soesoo, 1997), computational parameters of X_{PT} and Y_{PT} are obtained using formulas 1 and 2:

$$1) X_{PT} = 0.446 SiO_2 + 0.187 TiO_2 - 0.404 Al_2O_3 + 0.346 FeO_{Total} - 0.052 MnO + 0.309 MgO + 0.431 CaO - 0.446 Na_2O$$

$$2) Y_{PT} = -0.369 SiO_2 + 0.535 TiO_2 - 0.317 Al_2O_3 + 0.323 FeO_{Total} + 0.235 MnO - 0.516 MgO - 0.167 CaO - 0.153 Na_2O$$

The X_{PT} value for the investigated samples is in the range of 40 to 41.5 and the Y_{PT} is in the range of -30.34 to -30.29. According to the method (Soesoo, 1997), the temperature of the studied clinopyroxenes is in the range of 1150-1200°C (Fig. 8a). According to the calculations made by (Nimis and Taylor, 2000), the crystallization temperature of the studied clinopyroxenes is

656 to 1134°C with a change of ± 25 . These calculations are based on formula (3).

$$(3) T(^{\circ}K) = 23166 + 39.28 (P \text{ kbar} / 13.25 + 15.35 Ti + 4.5 Fe - 1.55 (Al + Cr - Na - K) + (\ln a^{CPX_{en}})^2$$

In the thermometry of clinopyroxene crystallization, the proposed formula (Putirka, 2008) for the studied samples of the clinopyroxene, estimates the crystallization temperature of 1267-1197°C. This formula is (4):

$$(4) T(^{\circ}K) = 93100 + 544 P(\text{Kbar}) / 61.1 + 36.6 X^{CPX_{Ti}} + 10.9 (X^{CPX_{Fe}} - 0.95 (X^{CPX_{Al}} + X^{CPX_{Cr}} - X^{CPX_{Na}} - X^{CPX_{K}}) + 0.395 [(\ln a^{CPX_{en}})]^2$$

The Hornblende- Clinopyroxene thermometry based on the equilibrium of Mg and Fe cations between the Hornblende and clinopyroxene minerals, is coexistence (Anderson, 1996). Using this method, the equilibrium temperature of these two minerals in the studied hornblende gabbro is 1000 to 1100°C (Fig. 8b). In the hornblende-plagioclase thermometry method, based on the method (Blundy and Holland, 1990), which is used at temperatures of 400 to 1000 °C and pressure of 1 kbar, the temperature is obtained according to the following formula 5:

$$T = \frac{0.667 - 48.98Y}{-0.0429 - 0.008314 \cdot \ln K} \quad K = \frac{(Si-4)}{(8-Si)} X_{Ab}^{plg}$$

The equilibrium temperature of the two hornblende-plagioclase minerals based on the pressure (Schmidt, 1992) is estimated at 548-450 °C. In the drawing diagram of the clinopyroxenes pressure determination (Soesoo, 1997), the crystallization pressure of the investigated pyroxenes is estimated 2-5 kbar (Fig. 8c). In the barometric method (Putirka, 2008), which is calculated based on formula (6), the distribution of Al between the clinopyroxene and the coexistent magma is important. According to this method, the pressure of the investigated samples is 2.05-5.58 kbar. In Formula 6, for each cation Al, six oxygen atoms are considered.

$$(6) P(\text{kbar}) = -57.9 + 0.0475T(K) - 40.6(X_{FeO}^{liq}) - 47.7(X_{CaTs}^{CPX}) + 0.676(X_{H_2O}^{liq}) - 153(X_{CaO_0.5}^{liq} X_{SiO_2}^{liq}) + 6.89[X_{Al}^{CPX} / X_{Al_2O_3}^{liq}]$$

$$X_{Al}^{CPX} = X_{Al}^{(IV)CPX} + X_{Al}^{(VI)CPX}$$

Based on the Al^t vs. $Fe^t/(Mg+Fe^t)$ in the studied amphiboles, a pressure is 4-6 kbar that is estimated by method (Schmidt, 1992) to crystallize the studied amphiboles (Fig. 8d).

According to the pressures of (Putirka, 2008), the depth of the gabbroic body crystallization is 14 km. In Fig. 9 the depth of the crystallization of the studied clinopyroxenes is 13 to 17 km, too.

3. CONCLUSION

Due to the percentage of the major minerals of plagioclase, pyroxene, and amphibole in the Dehsard gabbroic body, these rocks are hornblende gabbro. The clinopyroxenes are diopsides and of calcium-magnesium- iron clinopyroxene. The amphiboles of the area are magnesium hornblende and actinolite, and the plagioclases are albite-oligoclase. According to the chemical composition of clinopyroxenes and amphiboles, they have magmatic and sub-alkaline to calc-alkaline nature.

Thermometry and barometry based on the clinopyroxene mineral demonstrate a temperature of 1100 to 1200 °C and a pressure of 2.05 to 5.58 kbar in the low oxygen fugacity range for the crystallization of the studied clinopyroxenes. This pressure estimates a depth of about 14 km for the crystallization of the studied gabbroic body. The tectonic setting of parental magma of these minerals is the arc magma related to the subduction environment.

REFERENCES

- Agemar, T., Wörner, G., & Heumann, A. (1999). Stable isotopes and amphibole chemistry on hydrothermally altered granitoids in the North Chilean Precordillera: a limited role for meteoric water?. *Contributions to Mineralogy and Petrology*, 136(4), 331-344.
- Amini S., Moradpour N., ZareiSahamieh R., "Petrography, geochemistry and petrology of the South Sahneh Ophiolite Complex (NE Kermanshah)", Farsi). *Iranian Journal of Crystallography and mineralogy* 14(2)(2006) 225-246.
- Anderson, J. L. (1996). Status of thermobarometry in granitic batholiths. *Transactions of the Royal Society of Edinburgh*, 87, 125-138.
- Arvin, M., Pan, Y., Dargahi, S., Malekizadeh, A., & Babaei, A. (2007). Petrochemistry of the Siah-Kuh granitoid stock southwest of Kerman, Iran: Implications for initiation of Neotethys subduction. *Journal of Asian Earth Sciences*, 30(3-4), 474-489.
- Avanzinelli, R., Bindi, L., Menchetti, S., & Conticelli, S. (2004). Crystallisation and genesis of peralkaline magmas from Pantelleria Volcano, Italy: an integrated petrological and crystal-chemical study. *Lithos*, 73(1-2), 41-69.
- Aydin, F., Karsli, O., & Sadiklar, M. B. (2009). Compositional variations, zoning types and petrogenetic implications of low-pressure clinopyroxenes in the Neogene alkaline volcanic rocks of northeastern Turkey. *Turkish Journal of Earth Sciences*, 18(2), 163-186.
- Azizi, H., Asahara, Y., Mehrabi, B., & Chung, S. L. (2011). Geochronological and geochemical constraints on the petrogenesis of high-K granite from the Suffi abad area, Sanandaj-Sirjan Zone, NW Iran. *Geochemistry*, 71(4), 363-376.
- Baharifar, A., Moinevaziri, H., Bellon, H., & Piqué, A. (2004). The crystalline complexes of Hamadan (Sanandaj-Sirjan zone, western Iran): metasedimentary Mesozoic sequences affected by Late Cretaceous tectono-metamorphic and plutonic events. *Comptes Rendus Geoscience*, 336(16), 1443-1452.
- Beccaluva, L., Macciotta, G., Piccardo, G. B., & Zeda, O. (1989). Clinopyroxene composition of ophiolite basalts as petrogenetic indicator. *Chemical Geology*, 77(3-4), 165-182.
- Berberian, M. (2014). Active Tectonics and Geologic Setting of the Iranian Plateau. In *Developments in Earth Surface Processes* (Vol. 17, pp. 151-171). Elsevier.
- Berberian, M., & King, G. C. P. (1981). Towards a paleogeography and tectonic evolution of Iran. *Canadian journal of earth sciences*, 18(2), 210-265.
- Berger, J., Femenias, O., Mercier, J. C. C., & Demaiffe, D. (2005). Ocean-floor hydrothermal metamorphism in the Limousin ophiolites (western French Massif Central): evidence of a rare preserved Variscan oceanic marker. *Journal of Metamorphic geology*, 23(9), 795-812.
- Bindi, L., Cellai, D., Melluso, L., Conticelli, S., Morra, V., & Menchetti, S. (1999). Crystal chemistry of clinopyroxene from alkaline undersaturated rocks of the Monte Vulture Volcano, Italy. *Lithos*, 46(2), 259-274.
- Blundy, J. D., & Holland, T. J. (1990). Calcic amphibole equilibria and a new amphibole-plagioclase geothermometer. *Contributions to mineralogy and petrology*, 104(2), 208-224.
- Chivas, A. R. (1982). Geochemical evidence for magmatic fluids in porphyry copper mineralization. *Contributions to Mineralogy and Petrology*, 78(4), 389-403.
- Coltorti, M., Bonadiman, C., Faccini, B., Grégoire, M., O'Reilly, S. Y., & Powell, W. (2007). Amphiboles from suprasubduction and intraplate lithospheric mantle. *Lithos*, 99(1-2), 68-84.
- Deevsalar, R., Shinjo, R., Wang, K. L., Hadi, Y., & Neill, I. (2018). Gabbroic-dioritic dykes from the Sanandaj-Sirjan Zone: windows on Jurassic and Eocene geodynamic processes in the Zagros Orogen, western Iran. *Journal of the Geological Society*, 175(6), 915-933.
- Dorani M., Moradian A., "Geochemical and tectonomagmatic investigation of gabbros in southwest of Shahr-Babak, Kerman Province", *Iran Soc Cryst Mineral* 86 (2007) 193-210.
- Falcon, N. L. (1974). Southern Iran: Zagros Mountains. *Geological Society, London, Special Publications*, 4(1), 199-211.
- Ghasemi H., Derakhshi M., "Mineralogy, geochemistry and role of olivine mechanical separation in generation of Lower Paleozoic igneous rocks in Shirgesht area, NW of Tabas, Central Iran", *Iranian Journal of Crystallography and mineralogy* 16 (2008) 227-224.
- Ghorbani G., "Geothermobarometry and mineral chemistry of ferroanpargasite gabbroic cumulates in volcanic rocks from South of Shahrood", (2008).
- ELZ, R. T. (1973). Phase relations of basalts in their melting range at PH₂O= 5 kb as a function of oxygen fugacity: part I. Mafic phases. *Journal of Petrology*, 14(2), 249-302..
- Howie, R. A., Zussman, J., & Deer, W. (1992). *An introduction to the rock-forming minerals* (p. 696). Longman.
- Kamenetsky, V. S., Maas, R., Sushchevskaya, N. M., Norman, M. D., Cartwright, I., & Peyve, A. A. (2001). Remnants of Gondwanan continental lithosphere in oceanic upper mantle: Evidence from the South Atlantic Ridge. *Geology*, 29(3), 243-246.
- Le Bas, M. J. (1962). The role of aluminum in igneous clinopyroxenes with relation to their parentage. *American Journal of Science*, 260(4), 267-288.
- Leake, B. E., Woolley, A. R., Arps, C. E., Birch, W. D., Gilbert, M. C., Grice, J. D., ... & Linthout, K. (1997). Nomenclature of amphiboles; report of the Subcommittee on Amphiboles of the International Mineralogical Association Commission on new minerals and mineral names. *Mineralogical magazine*, 61(405), 295-310.
- Leterrier, J., Maury, R. C., Thonon, P., Girard, D., & Marchal, M. (1982). Clinopyroxene composition as a method of identification of the magmatic affinities of paleo-volcanic series. *Earth and Planetary Science Letters*, 59(1), 139-154.

28. Loucks, R. R. (1990). Discrimination of ophiolitic from nonophiolitic ultramafic-mafic allochthons in orogenic belts by the Al/Ti ratio in clinopyroxene. *Geology*, 18(4), 346-349.
29. Mohajjel, M., Fergusson, C. L., & Sahandi, M. R. (2003). Cretaceous-Tertiary convergence and continental collision, Sanandaj-Sirjan zone, western Iran. *Journal of Asian Earth Sciences*, 21(4), 397-412.
30. Mohammadi, N., Sodoudi, F., Mohammadi, E., & Sadidkhouy, A. (2013). New constraints on lithospheric thickness of the Iranian plateau using converted waves. *Journal of seismology*, 17(3), 883-895. [16] Gill R., "Igneous rocks and processes: a practical guide", John Wiley & Sons (2010).
31. Molina, J. F., Scarrow, J. H., Montero, P. G., & Bea, F. (2009). High-Ti amphibole as a petrogenetic indicator of magma chemistry: evidence for mildly alkalic-hybrid melts during evolution of Variscan basic-ultrabasic magmatism of Central Iberia. *Contributions to Mineralogy and Petrology*, 158(1), 69-98.
32. Morimoto, N. (1988). Nomenclature of pyroxenes. *Mineralogy and Petrology*, 39(1), 55-76.
33. Nazemei M, Arvin M., & Dargahi S., (2018). Geochemistry and source characteristics of Dehsard mafic volcanic rocks in the southeast of the Sanandaj-Sirjan zone, Iran: implications for the evolution of the Neo-Tethys Ocean, *Turkish Journal of Earth Sciences*. 27, 249-268.
34. Nazemzadeh, M., & Rashidi, A. (2006). Geological map of the Dehsard (Bezar), Scale 1/100,000. *Geological Survey of Iran, Sheet*, (7347).
35. Nimis, P., & Taylor, W. R. (2000). Single clinopyroxene thermobarometry for garnet peridotites. Part I. Calibration and testing of a Cr-in-Cpx barometer and an enstatite-in-Cpx thermometer. *Contributions to Mineralogy and Petrology*, 139(5), 541-554.
36. Nisbet, E. G., & Pearce, J. A. (1977). Clinopyroxene composition in mafic lavas from different tectonic settings. *Contributions to mineralogy and petrology*, 63(2), 149-160.
37. Omrani, J., Agard, P., Whitechurch, H., Benoit, M., Prouteau, G., & Jolivet, L. (2008). Arc-magmatism and subduction history beneath the Zagros Mountains, Iran: a new report of adakites and geodynamic consequences. *Lithos*, 106(3-4), 380-398.
38. Paplke J., Cameron K., Baldwin K., (1974). Amphiboles and pyroxenes: characterization of other than quadrilateral components and estimates of ferric iron from microprobe data, Geol. Soc. *Amer. Abstracts*, 1053-1054.
39. Putirka, K. D. (2008). Thermometers and barometers for volcanic systems. *Reviews in mineralogy and geochemistry*, 69(1), 61-120.
40. Rahgoshai M., Shafaei, M.H., Pirasteh, S., "The distinctive trace elements signature of the less-evolved MORB materials in the south of Birjand ophiolites", (2007).
41. Sadeghian, M., & Minggou, Z. (2019). Mineral chemistry and Thermobarometry of Middle Jurassic diabasic dikes Cutting metamorphic-igneous Shotor-Kuh complex (SE Shahrood). *Iranian Journal of Crystallography and Mineralogy*, 26(4), 915-928.
42. Schmidt, M. W. (1992). Amphibole composition in tonalite as a function of pressure: an experimental calibration of the Al-in-hornblende barometer. *Contributions to mineralogy and petrology*, 110(2-3), 304-310.
43. Schweitzer, E. L., Papike, J. J., & Bence, A. E. (1979). Statistical analysis of clinopyroxenes from deep-sea basalts. *American Mineralogist*, 64(5-6), 501-513..
44. Sedighian, S., Dargahi, S., & Arvin, M. (2017). Petrochemistry of Khunrang intrusive complex, southeast of Kerman, Iran: Implications for magmatic evolution of Sanandaj-Sirjan zone in the Mesozoic time. *Journal of African Earth Sciences*, 134, 149-165.
45. Sepahi, A. A., & Athari, S. F. (2006). Petrology of major granitic plutons of the northwestern part of the Sanandaj-Sirjan Metamorphic Belt, Zagros Orogen, Iran: with emphasis on A-type granitoids from the SE Saqqez area. *Neues Jahrbuch für Mineralogie-Abhandlungen: Journal of Mineralogy and Geochemistry*, 183(1), 93-106.
46. Shahbazi, H., Siebel, W., Pourmoafee, M., Ghorbani, M., Sepahi, A. A., Shang, C. K., & Abedini, M. V. (2010). Geochemistry and U-Pb zircon geochronology of the Alvand plutonic complex in Sanandaj-Sirjan Zone (Iran): New evidence for Jurassic magmatism. *Journal of Asian Earth Sciences*, 39(6), 668-683.
47. Shelley, D. (1993). *Igneous and metamorphic rocks under the microscope: classification, textures, microstructures and mineral preferred-orientations* (No. 552.3/. 4 SHE).
48. Sial, A. N., Ferreira, V. P., Fallick, A. E., & Cruz, M. J. M. (1998). Amphibole-rich clots in calc-alkalic granitoids in the Borborema province, northeastern Brazil. *Journal of South American Earth Sciences*, 11(5), 457-471.
49. Soesoo, A. (1997). A multivariate statistical analysis of clinopyroxene composition: Empirical coordinates for the crystallisation PT-estimations. *GFF*, 119(1), 55-60.
50. Stoecklin, J. (1968). Structural history and tectonics of Iran: a review. *AAPG bulletin*, 52(7), 1229-1258.
51. Zhu, Y., & Ogasawara, Y. (2004). Clinopyroxene phenocrysts (with green salite cores) in trachybasalts: implications for two magma chambers under the Kokchetav UHP massif, North Kazakhstan. *Journal of Asian Earth Sciences*, 22(5), 517-527.

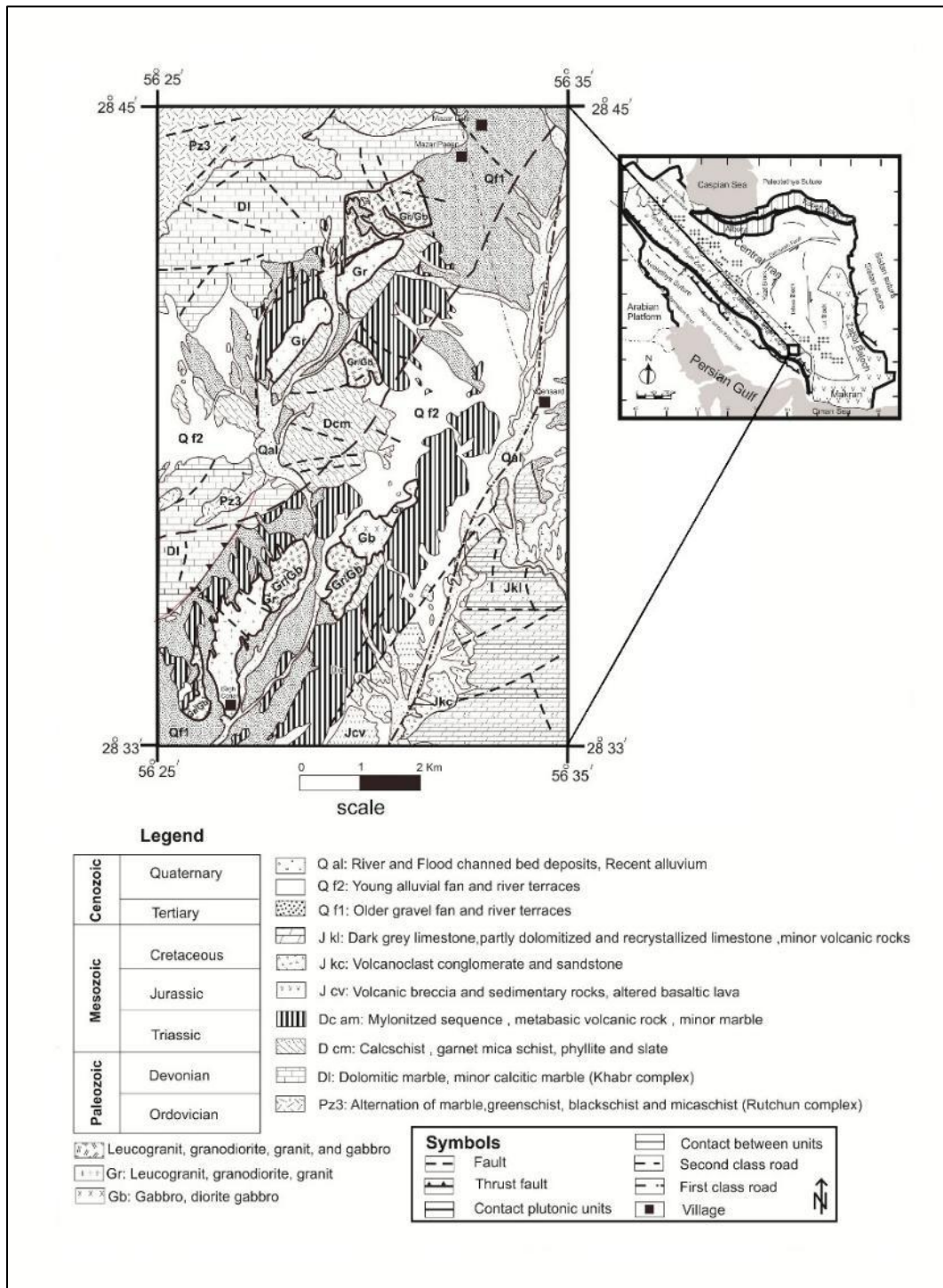


Fig. 1. Geologic map of gabbroic rocks of the study area [25].

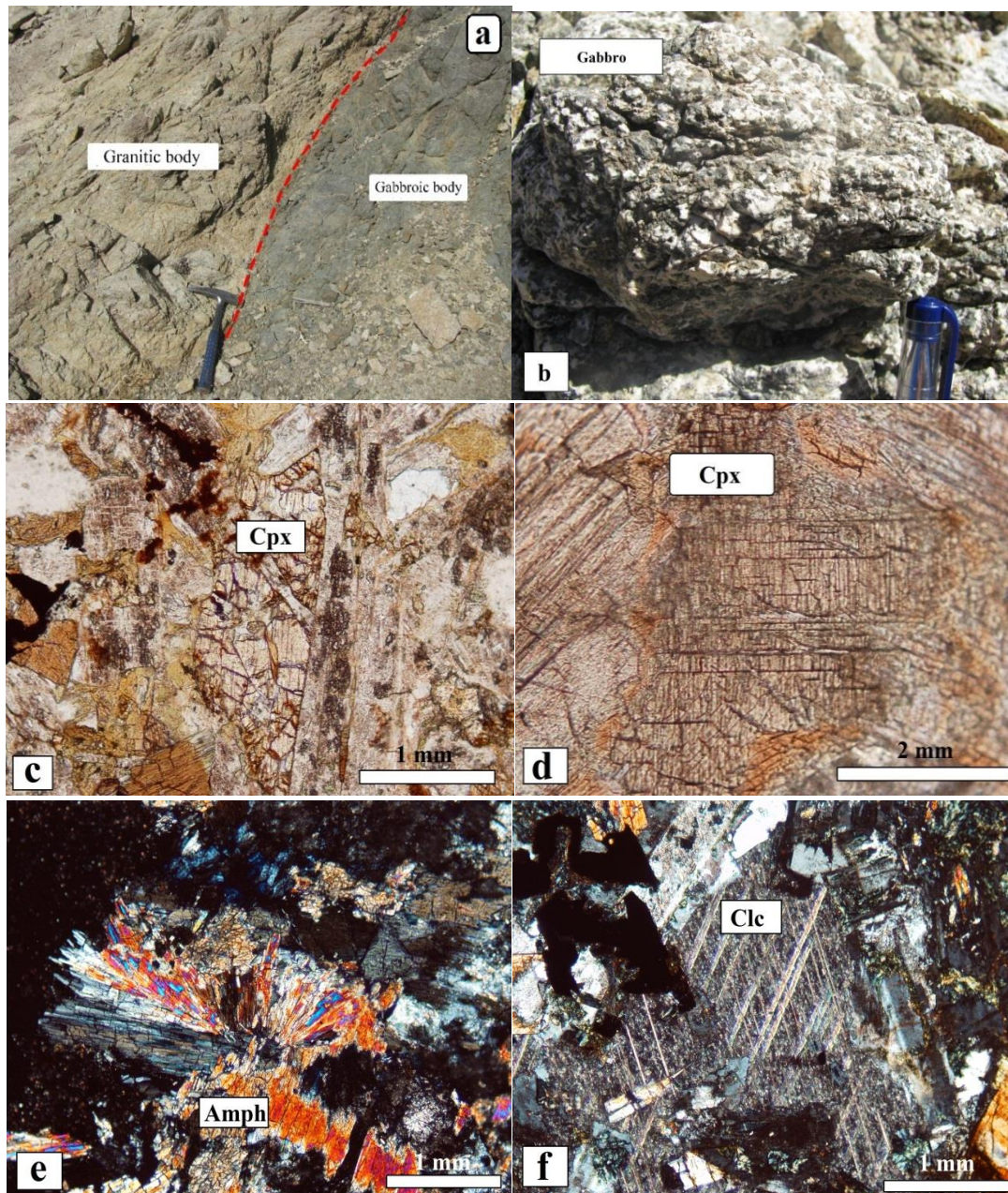


Fig. 2. a) The felsic and mafic bodies in the Dehsard area, b) The mesocratic gabbroic rocks, c and e) The granular texture in hornblende gabbro, d) The cleavage of pyroxene in gabbro, f) calcite as a secondary mineral in gabbroic rocks.

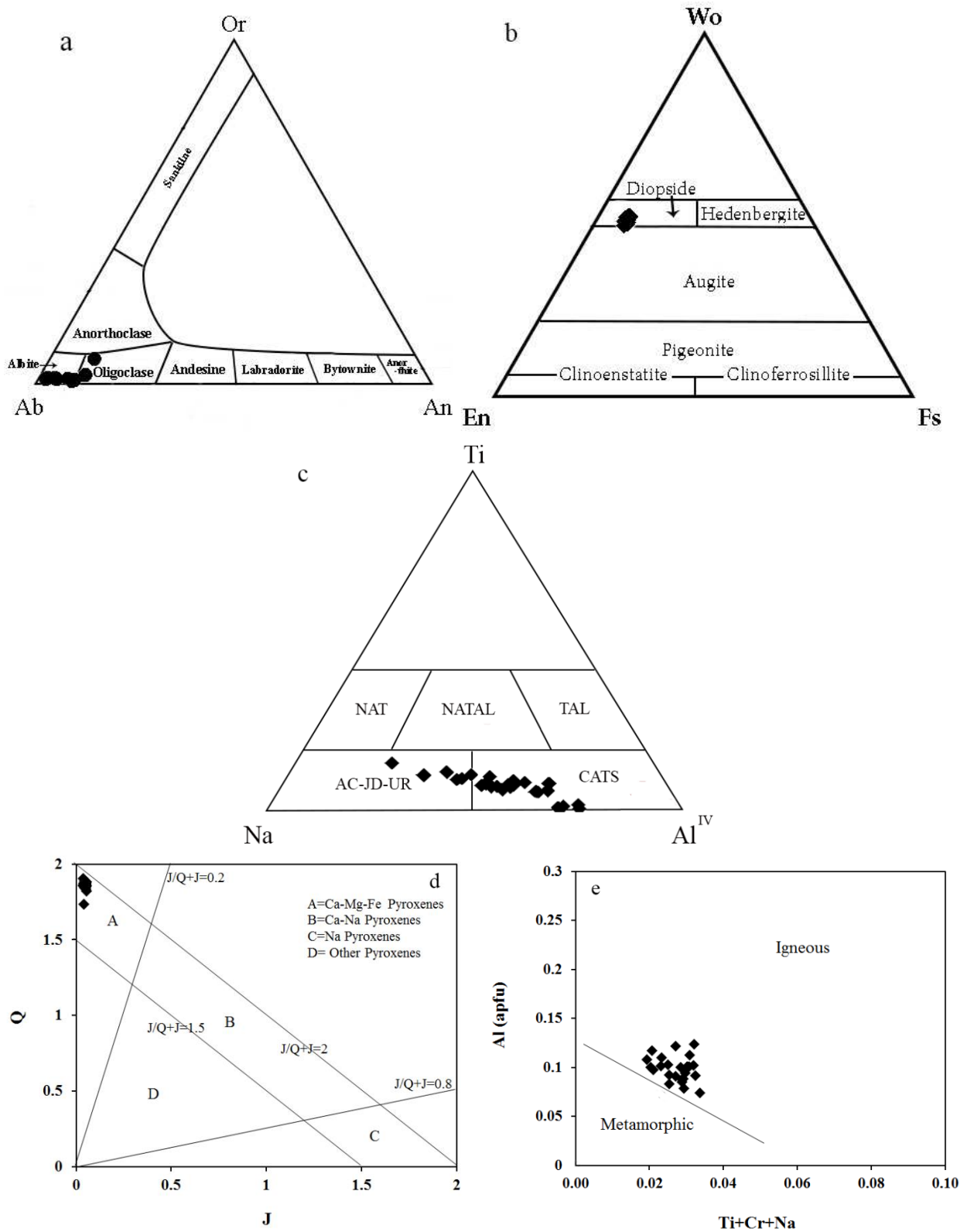


Fig. 3. a) Classification ternary diagram for feldspar (Ab–An–Or plot; 31), Classification and discriminant diagrams for clinopyroxene (after 27) of the studied gabbroic rocks: b) En–Wo–Fs ($Mg_2Si_2O_6$ – $Ca_2Si_2O_6$ – $Fe_2Si_2O_6$) plot, c) Ti–Na–Al^{IV} diagram, d) Q–J (Q=Ca+Mg+Fe²⁺, J=2Na)[27], e) the Al^{tot} vs Ti+Cr+Na diagram (29).

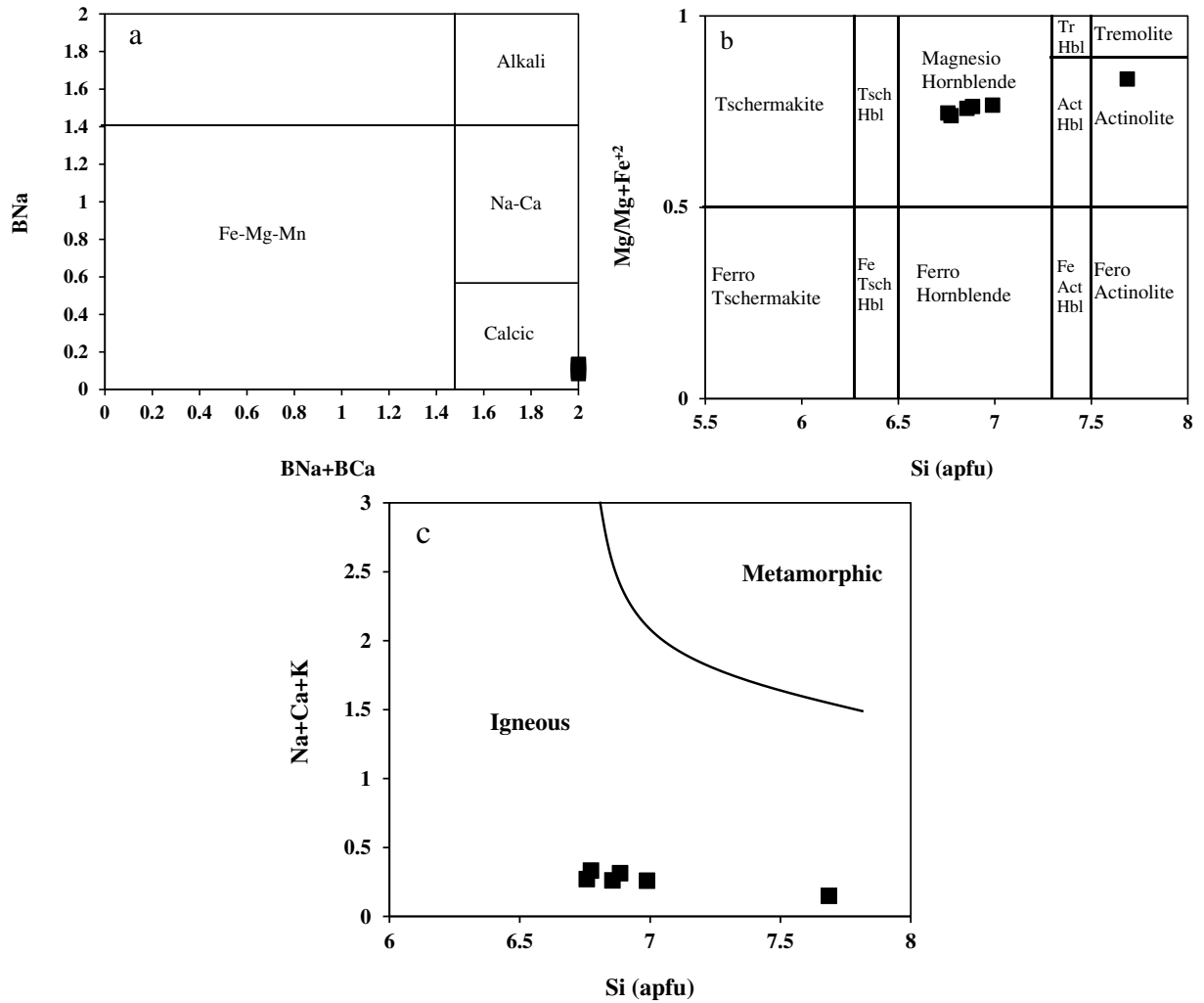


Fig. 4. Classification diagram of amphibole of the studied gabbroic rocks a) Bca+BNa vs. BNa diagram, b) Si vs. Mg/(Mg+Fe²⁺) diagram (32), c) Si vs. Na+Ca+K diagram (33).

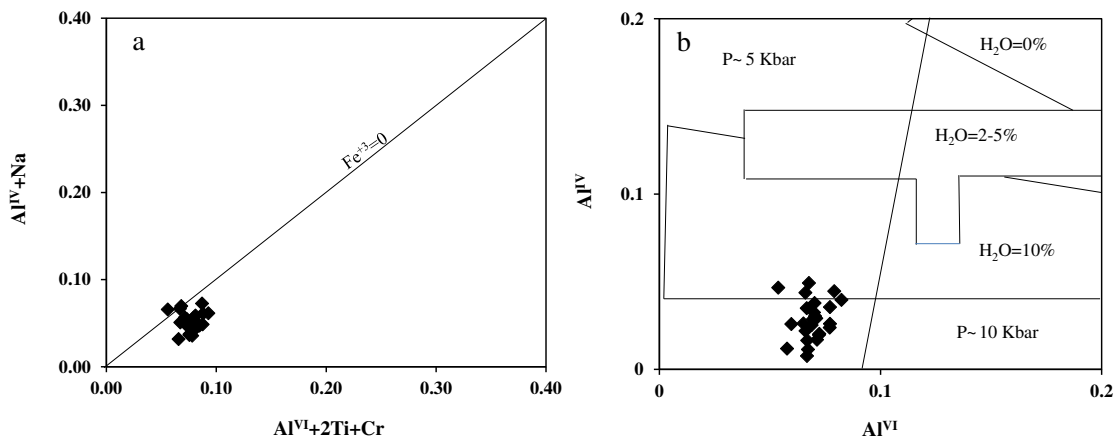


Fig. 5. a) Al^{VI}+2Ti+Cr vs. Al^{IV}+Na diagram (35), b) Al^{VI} vs. Al^{IV} diagram (36).

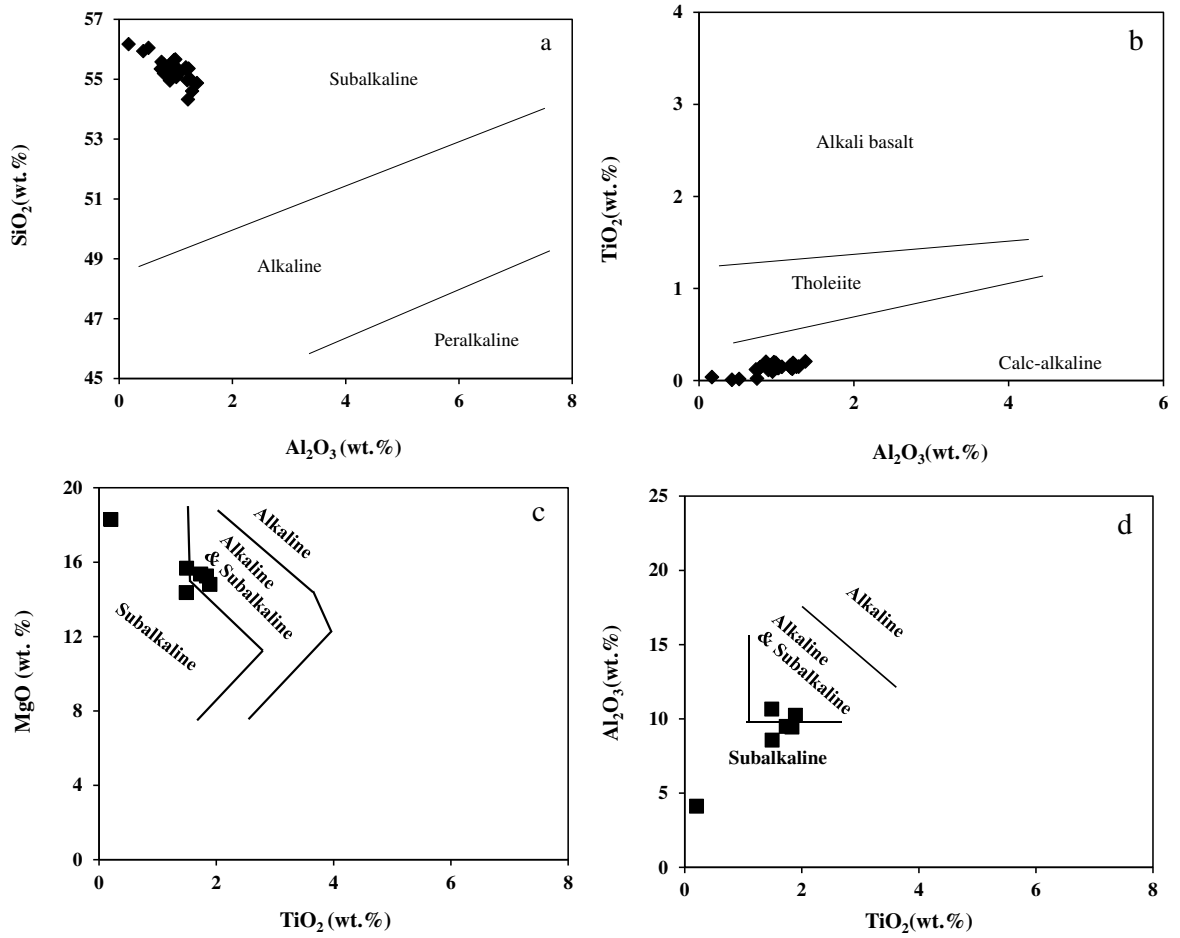
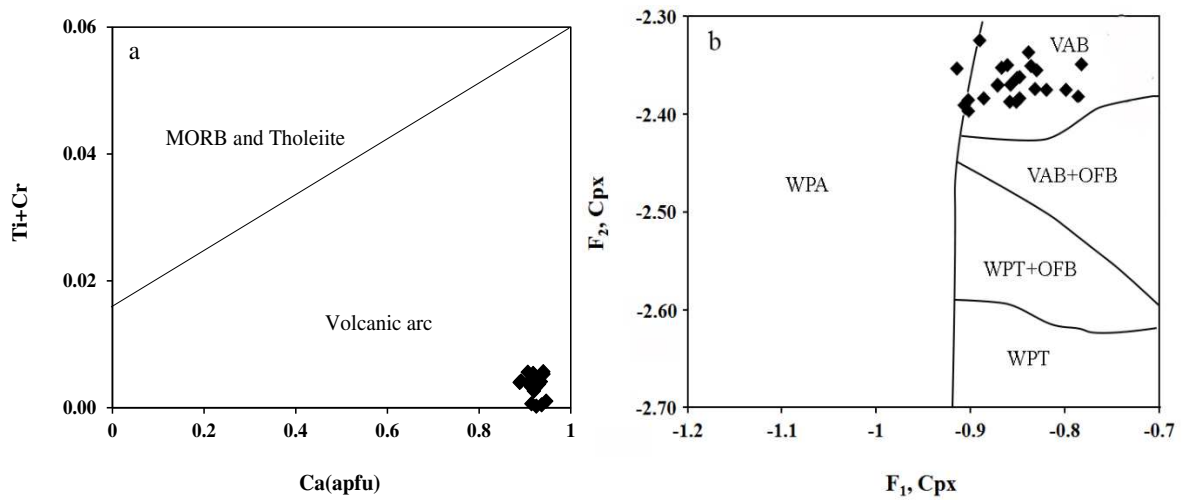


Fig. 6. The discriminant diagrams for clinopyroxene a and b) Al_2O_3 Vs SiO_2 and TiO_2 [41]. The discriminant diagrams for amphibole c and d) TiO_2 vs. Al_2O_3 and MgO [19].



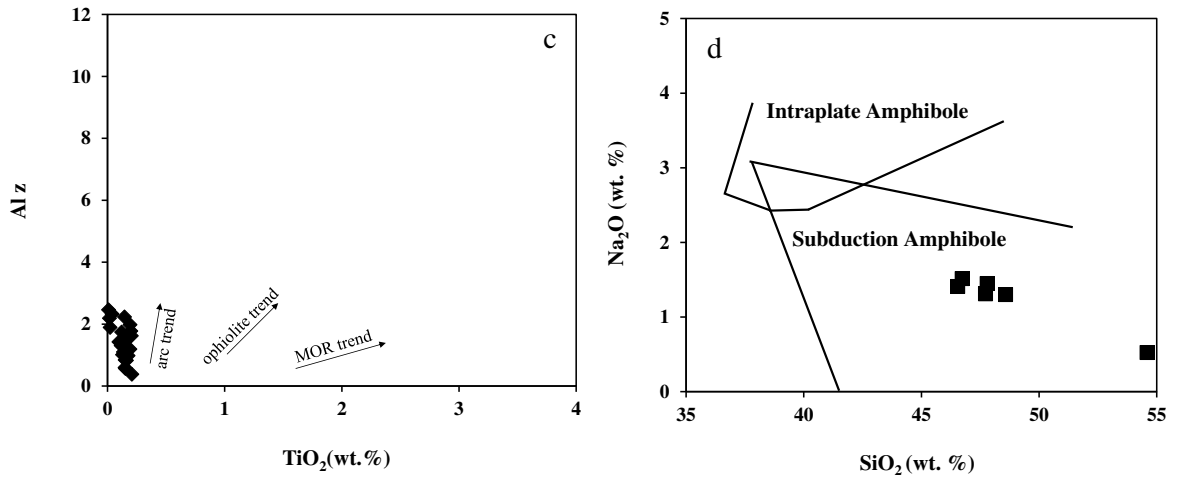


Fig. 7. a) Ca vs. Ti+Cr diagram [39], b) F1 - F2 (41), c) TiO₂ vs. Al₂O₃ diagram (42), d) SiO₂-Na₂O diagram (43).

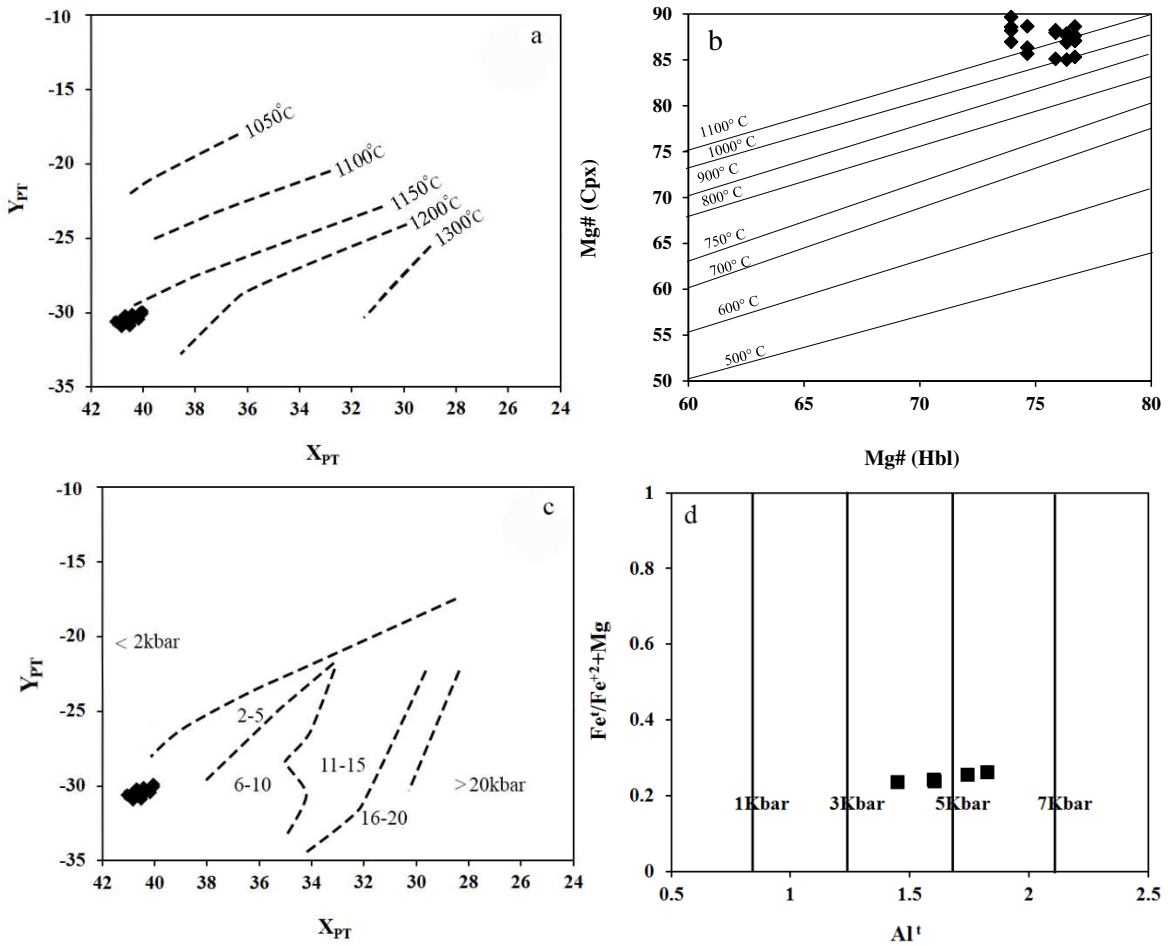


Fig. 8. a) The estimation of studied clinopyroxenes temperature base on Soesoo (47) diagram, b) The Hornblende- Clinopyroxene thermometry based on Anderson (50) diagram, c) X_{PT}-Y_{PT} diagram (47), d) Al^I vs. Fe^I/(Mg+Fe^I) (52).

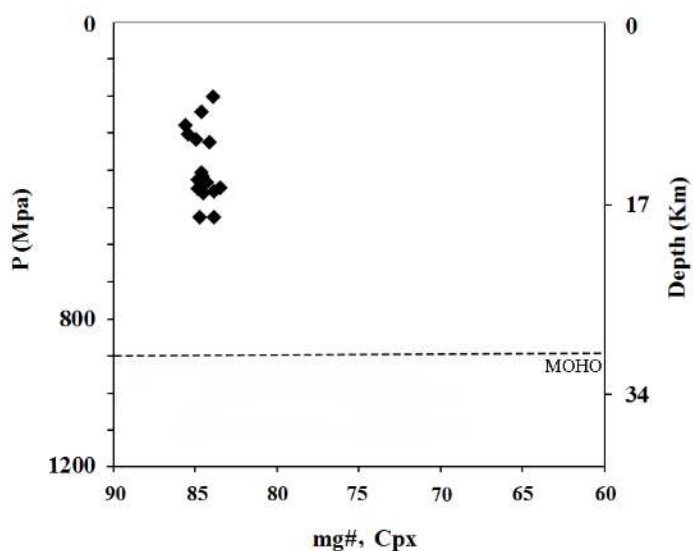


Fig. 9. Pressure estimates according to [49] in the study area.

Table 1. Representative chemical composition and calculated mineral formulae of plagioclases of gabbroic rocks of the study area. Formulae was calculated on the basis of 8 oxygens.

sample	1-8	1-9	2-7	2-8	2-9	2-10	4-6	4-7	4-8	6-5
SiO ₂ (wt.%)	71/67	71/68	72/45	71/32	67/36	72/21	71/97	70/61	70/07	73/43
Al ₂ O ₃	20/66	19/58	21/01	21/34	25/08	20/79	20/62	22/17	21/77	20/85
FeO	0/00	0/05	0/00	0/00	0/06	0/00	0/13	0/07	0/14	0/00
CaO	0/15	0/42	0/92	0/84	0/38	0/94	0/18	1/24	1/24	0/31
Na ₂ O	7/52	6/47	6/84	6/90	5/63	8/71	7/43	6/64	7/24	6/23
K ₂ O	0/08	0/06	0/04	0/02	2/59	0/10	0/09	0/79	0/24	0/09
Total	100/07	98/26	101/27	100/42	101/10	102/75	100/43	101/52	100/70	100/92
Si(apfu)	2/86	2/92	2/86	2/84	2/66	2/81	2/87	2/78	2/78	2/91
Al	1/10	1/06	1/11	1/13	1/32	1/08	1/09	1/16	1/15	1/10
Fe	0/00	0/00	0/00	0/00	0/00	0/00	0/01	0/01	0/01	0/00
Ca	0/01	0/03	0/07	0/07	0/03	0/07	0/01	0/10	0/10	0/02
Na	1/20	1/05	1/08	1/10	0/89	1/36	1/18	1/05	1/15	0/99
K	0/01	0/01	0/01	0/00	0/41	0/02	0/02	0/12	0/04	0/01
Or	1/02	0/95	0/61	0/31	30/80	1/05	1/24	9/80	2/96	1/40
Ab	98/03	95/93	93/12	93/98	66/93	93/89	97/56	82/47	89/41	96/19
An	0/95	3/12	6/28	5/71	2/27	5/06	1/21	7/72	7/63	2/41

Table 2. Representative chemical composition and calculated mineral formulae of clinopyroxenes of gabbroic rocks of the study area.

Sample (wt.%)	SiO ₂	TiO ₂	Al ₂ O ₃	FeO	MnO	MgO	CaO	Na ₂ O	K ₂ O	Total
1-1	55/20	0/15	0/79	4/92	0/18	15/11	22/60	0/39	0/00	99/33
1-2	55/58	0/02	0/75	4/17	0/18	15/66	23/47	0/27	0/00	100/10
1-3	56/17	0/04	0/17	4/83	0/17	15/14	24/42	0/27	0/00	101/21
1-4	55/94	0/01	0/42	4/54	0/25	15/25	23/75	0/29	0/00	100/45
1-5	55/44	0/14	0/97	4/56	0/22	15/47	23/40	0/35	0/00	100/56
1-6	54/96	0/12	0/90	4/54	0/17	15/23	23/57	0/34	0/00	99/82
2-1	54/61	0/15	1/29	4/63	0/15	15/77	22/75	0/36	0/00	99/71
2-2	56/05	0/02	0/52	4/18	0/20	15/33	24/17	0/33	0/00	100/79

2-4	55/34	0/14	1/19	4/54	0/14	15/30	23/62	0/30	0/00	100/57
3-5	55/19	0/20	0/86	5/03	0/21	15/15	23/21	0/37	0/00	100/23
3-6	55/19	0/17	0/93	4/45	0/17	15/36	23/43	0/37	0/00	100/06
3-7	55/64	0/20	0/97	4/56	0/16	15/22	23/66	0/36	0/00	100/77
4-1	55/36	0/18	1/23	4/86	0/24	15/15	23/66	0/39	0/00	101/07
4-2	55/35	0/14	1/03	4/83	0/16	15/10	23/95	0/36	0/00	100/91
4-3	55/50	0/14	0/79	4/49	0/21	15/48	23/82	0/36	0/02	100/81
4-4	55/35	0/12	0/73	4/45	0/16	15/56	23/40	0/28	0/00	100/05
4-5	54/97	0/13	1/20	4/67	0/17	15/22	23/50	0/31	0/02	100/18
5-1	55/49	0/10	0/95	4/77	0/17	15/30	23/73	0/26	0/01	100/77
5-2	55/08	0/14	1/01	4/58	0/18	15/23	23/53	0/37	0/02	100/11
5-5	55/40	0/16	1/18	4/55	0/18	15/43	23/95	0/30	0/02	101/16
5-6	55/21	0/15	1/07	4/46	0/10	15/55	24/13	0/29	0/00	100/97
6-1	55/67	0/19	0/99	4/73	0/20	15/01	23/67	0/31	0/00	100/78
6-2	54/32	0/19	1/21	4/49	0/17	14/55	23/79	0/35	0/00	99/08
6-3	55/00	0/15	1/26	4/84	0/18	14/81	24/02	0/36	0/00	100/61
6-4	54/88	0/21	1/37	4/86	0/22	14/82	24/15	0/40	0/01	100/91

Table 2. Continued Formulae calculated on the basis of 6 oxygen.

Sample (apfu)	Si	Al	Ti	Mg	Fe	Ca	Na	K	Al ^(IV)	Al ^(VI)	mg#	En	Fs	Wo
1-1	2/03	0/12	0/00	0/83	0/11	0/89	0/03	0/00	0/04	0/08	88/52	44/15	8/37	47/48
1-2	2/02	0/11	0/00	0/85	0/10	0/91	0/02	0/01	0/04	0/07	89/67	44/79	6/98	48/24
1-3	2/03	0/10	0/00	0/82	0/14	0/95	0/02	0/00	0/05	0/05	85/03	42/65	7/90	49/44
1-4	2/03	0/12	0/00	0/83	0/12	0/92	0/02	0/00	0/05	0/07	87/09	43/57	7/67	48/76
1-5	2/01	0/10	0/00	0/84	0/11	0/91	0/02	0/01	0/03	0/07	88/66	44/23	7/69	48/09
1-6	2/01	0/09	0/00	0/83	0/11	0/92	0/02	0/00	0/03	0/07	87/96	43/75	7/60	48/65
2-1	2/00	0/08	0/00	0/86	0/08	0/89	0/03	0/01	0/01	0/07	91/18	45/31	7/71	46/98
2-2	2/03	0/11	0/00	0/83	0/12	0/94	0/02	0/01	0/04	0/07	86/97	43/60	6/99	49/40
2-4	2/00	0/10	0/00	0/82	0/11	0/92	0/02	0/00	0/03	0/08	88/64	43/84	7/52	48/65
3-5	2/01	0/10	0/01	0/82	0/12	0/91	0/03	0/00	0/03	0/07	87/49	43/57	8/46	47/97
3-6	2/01	0/10	0/00	0/83	0/11	0/91	0/03	0/00	0/03	0/07	88/59	44/15	7/45	48/40
3-7	2/01	0/11	0/01	0/82	0/12	0/92	0/03	0/00	0/04	0/08	87/62	43/65	7/60	48/75
4-1	2/00	0/09	0/00	0/82	0/12	0/92	0/03	0/00	0/02	0/07	87/08	43/26	8/18	48/56
4-2	2/01	0/09	0/00	0/82	0/13	0/93	0/03	0/00	0/02	0/07	86/34	43/00	7/97	49/02
4-3	2/01	0/09	0/00	0/83	0/11	0/92	0/03	0/00	0/03	0/06	88/23	43/93	7/49	48/59
4-4	2/02	0/10	0/00	0/85	0/10	0/91	0/02	0/01	0/03	0/07	89/17	44/51	7/39	48/09
4-5	2/00	0/09	0/00	0/83	0/11	0/92	0/02	0/00	0/02	0/07	88/20	43/70	7/80	48/50
5-1	2/01	0/10	0/00	0/82	0/11	0/92	0/02	0/00	0/03	0/07	87/87	43/56	7/89	48/56
5-2	2/01	0/09	0/00	0/83	0/12	0/92	0/03	0/01	0/03	0/07	87/64	43/75	7/66	48/59
5-5	2/00	0/08	0/00	0/83	0/11	0/93	0/02	0/00	0/02	0/07	88/07	43/71	7/52	48/77
5-6	1/95	0/07	0/00	0/82	0/00	0/91	0/02	0/09	0/01	0/06	0/00	43/86	7/23	48/91
6-1	2/01	0/12	0/01	0/81	0/12	0/92	0/02	0/00	0/04	0/08	86/90	43/14	7/96	48/90
6-2	2/00	0/10	0/01	0/80	0/14	0/94	0/02	0/01	0/02	0/08	85/32	42/47	7/63	49/90
6-3	2/00	0/09	0/00	0/80	0/13	0/93	0/03	0/00	0/02	0/07	85/67	42/45	8/07	49/48
6-4	1/99	0/07	0/01	0/80	0/14	0/94	0/03	0/01	0/01	0/07	85/11	42/30	8/14	49/56

Table 3. Representative chemical composition and calculated mineral formulae of amphiboles of gabbroic rocks of the study area. Formulae was calculated on the basis of 23 oxygens, $Mg\# = Mg / (Fe^{2+} + Mg)$.

sample	3-1	3-2	3-3	3-4	5-7	5-8
SiO ₂ (wt.%)	54.59	46.54	47.72	48.57	46.73	47.79
TiO ₂	0.20	1.49	1.83	1.49	1.89	1.73
Al ₂ O ₃	4.12	10.66	9.45	8.57	10.24	9.49
FeO	6.43	9.02	8.43	8.49	8.97	8.71
MnO	0.11	0.17	0.10	0.12	0.12	0.20
MgO	18.29	14.37	15.26	15.67	14.81	15.36
CaO	12.57	11.96	12.10	12.23	12.37	12.39
Na ₂ O	0.52	1.41	1.31	1.30	1.52	1.45
K ₂ O	0.25	1.06	1.00	0.78	1.01	0.90
Total	97.10	96.68	97.19	97.24	97.65	98.04
Si(apfu)	7.69	6.77	6.88	6.99	6.76	6.86
Ti	0.00	0.00	0.00	0.00	0.00	0.00
Al	0.68	1.83	1.61	1.45	1.75	1.60
Al ^(IV)	0.31	1.23	1.12	1.01	1.24	1.14
Al ^(VI)	0.37	0.60	0.49	0.44	0.50	0.46
Fe ²⁺	0.76	1.10	1.02	1.02	1.08	1.04
Mn	0.09	0.08	0.07	0.07	0.03	0.03
Mg	2.17	1.95	2.32	2.95	3.05	3.22
Ca	1.90	1.86	1.87	1.88	1.92	1.90
Na	0.14	0.40	0.37	0.36	0.42	0.40
K	0.05	0.20	0.18	0.14	0.19	0.17
B: Ca	1.90	1.86	1.87	1.88	1.92	1.90
B: Na	0.10	0.14	0.13	0.12	0.08	0.10
mg#	0.84	0.74	0.76	0.77	0.75	0.76